Isı Bilimi ve Tekniği Dergisi, 42, 1, 123-140, 2022
J. of Thermal Science and Technology
©2022 TIBTD Printed in Turkey
ISSN 1300-3615
https://doi.org/10.47480/isibted.1107486

DESIGN FIRE CURVE SELECTION OF SMALL SCALE POOL FIRES IN A SCALED METRO STATION

Umut Baris YILMAZ*, Oguz TURGUT, Nuri YUCEL***, Muhammed İlter BERBEROĞLU******
*Yuksel Proje A.S., Birlik Mahallesi 450. Cadde No: 23, 06610 Cankaya, Ankara / Turkey
barisyilmaz@yukselproje.com.tr, ORCID: 0000-0002-6103-7670
,*Gazi University, Faculty of Engineering, Department of Mechanical Engineering
06570 Maltepe, Ankara, Turkey
**oturgut@gazi.edu.tr, ORCID: 0000-0001-5480-1039
***nuyucel@gazi.edu.tr, ORCID: 0000-0001-9390-5877
****Turkish Aerospace Industry, Kahramankazan, Ankara, Turkey
milterx@yahoo.com, ORCID: 0000-0003-2957-5185

(Geliş Tarihi: 24.10.2021, Kabul Tarihi: 12.04.2022)

Abstract: n-heptane pool fire was numerically and experimentally investigated in a 1:100 scaled metro station. Fire Dynamics Simulator (FDS v6.7.5) has been applied to investigate smoke and temperature distribution by implementing different design curves in the station. Experimental and numerical studies were performed for 10 ml n-heptane fuel under zero piston effect. To develop performance-based design and to obtain reliable fire simulation results for structures, reasonable input conditions are essential for numerical studies. The aim of the study is to select most suitable fire design curve and make the numerical study independent of the experimental results for small scale hydrocarbon pool fires. In this study, t^2, tanh, Eurocode 1 (BS EN 1991-1-2), exponential, and quadratic fire curves were investigated and validated with experimental results. The numerical results obtained using FDS were validated with experimental data and good agreement was observed for all design fire curves except quadratic one. It was observed that the exponential design fire curve predicted more similarly to the experimental data over the fire duration including growth, fully developed and decay phases. Regardless of the experimental results, it was seen that the temperature distribution results obtained from the numerical study using exponential fire design curve and the radiation / turbulence parameters obtained from the literature were found to have an average of 5% difference with the experimental results. It was also seen that the t^2 and tanh curves have acceptable differences of 6.92% and 9.02%, respectively, and the Eurocode HC is less suitable than the other curves with a difference of 12.17%. Therefore, it can be said that in small scale hydrocarbon pool fires, fire design can be done using exponential design curve.
Keywords: Fire development, Design fire curve, Pool fire, N-heptane, Fire dynamics simulator (FDS)

ÖLÇEKLENDİRİLMİŞ BİR METRO İSTASYONUNDA KÜÇÜK ÖLÇEKLİ SIVI HAVUZ YANGINLARININ YANGIN TASARIM EĞRİSİ SEÇİMİ

Özet: n-heptan havuz yangını 1:100 ölçekli bir metro istasyonunda sayısal ve deneysel olarak incelenmiştir. Fire Dynamics Simulator (FDS v6.7.5) yazılımı ile istasyonda farklı tasarım eğrileri uygulanarak duman ve sıcaklık dağılımı araştırılmıştır. Sıfır piston etkisi altında 10 ml n-heptan yakıt için deneysel ve sayısal çalışmalar yapılmıştır. Performansa dayalı tasarımı geliştirmek ve yapılar için güvenilir yangın simülasyon sonuçları elde etmek için sayısal çalışmalarda güvenilir girdiler tanımlamak gerekmektedir. Çalışmanın amacı, küçük ölçekli hidrokarbon havuz yangınları için en uygun yangın tasarım eğrisini seçmek ve sayısal çalışmayı deneysel sonuçlardan bağımsız hale getirmektir. Bu çalışmada, t^2, tanh, Eurocode 1 (BS EN 1991-1-2), eksponansiyel ve ikinci dereceden yangın eğrileri incelenmiş ve deneysel sonuçlarla doğrulanmıştır. FDS kullanılarak elde edilen sayısal sonuçlar deneysel verilerle doğrulanmış ve ikinci dereceden hariç tüm yangın tasarım eğrileri ile uyumlu olduğu gözlenmiştir. Yangın süresi

boyunca büyüme, tam gelişme ve bozunma aşamalarını içeren eksponansiyel yangın tasarımı eğrisinin deneysel verilere daha yakın sonuçlar verdiği gözlemlenmiştir. Deneysel sonuçlardan bağımsız olarak, eksponansiyel yangın tasarım eğrisi kullanılarak yapılan sayısal çalışmadan elde edilen sıcaklık dağılım sonuçları ile literatürden elde edilen radyasyon/türbülans parametrelerinin deneysel sonuçlarla ortalama %5 farklılık gösterdiği görülmüştür. Ayrıca t^2 ve tanh yangın tasarım eğrilerinin de deneysel sonuçlarla %6.92 ve %9.02 gibi kabul edilebilir farklılıklar gösterdiği, Eurocode HC'nin ise %12.17'lik fark ile daha uzak olduğu gözlenmiştir. Bu nedenle küçük ölçekli hidrokarbon havuz yangınlarında eksponansiyel tasarım eğrisi kullanılarak yangın tasarımının yapılabileceği söylenebilir.
Anahtar Kelimler: Yangın gelişimi, Yangın tasarım eğrisi, Havuz yangını, N-heptan, Fire dynamics simulator (FDS)

NOMENCLATURE

C_p	Specific heat of air, $J \cdot kg^{-1} \cdot K^{-1}$
C_V	Deardorff model constant, -
D*	Characteristic fire diameter, m
D_F	Diffusivity of the fuel, $m^2 \cdot s^{-1}$
D_l	Material diffusivity, $m^2 \cdot s^{-1}$
f	Fuel, -
g	Acceleration of gravity, $m \cdot s^{-2}$
$\tilde{h}$	Favre-filtered enthalpy, $m^2 \cdot s^{-2}$
k	Time width coefficient, -
k_c	Thermal conductivity, W/m.K
k_{sgs}	Turbulent kinetic energy, $m^2 \cdot s^{-2}$
L_f	Flame height, m
n	Retard index, -
P	Pressure, Pa
r	Amplitude, -
q^r	Radiative heat flux, $W \cdot m^{-2}$
$\dot{Q}$	Peak heat release rate, kW
$\dot{Q}^*$	Fire Froude number, -
S_L	Flame spread, $m \cdot s^{-1}$
t	Time, s
T	Temperature, K
T_∞	Temperature of air, K
u,v,w	Three components of velocity vectors, $m \cdot s^{-1}$
$\bar{u}$	Average value of u at the grid cell center, $m \cdot s^{-1}$
$\hat{\bar{u}}$	Weighted average of u over the adjacent cells, $m \cdot s^{-1}$
$\tilde{u}$	Favre-filtered velocity, $m \cdot s^{-1}$
U	Overall heat transfer coefficient, $W \cdot m^{-2} \cdot K^{-1}$
$\overline{\dot{w}_l}$	Favre-filtered species source term, -
y_s	Soot yield, $kg \cdot kg^{-1}$
$\tilde{Y}_l$	Favre-filtered mass species concentration, $kg \cdot m^{-3}$

Greek Letters:

α	Fire growth rate, $kW \cdot s^2$
β_d	Ratio between the integrated energy at time td, (E_{tot}, t_d) and total energy released in the fire (E_{tot})
μ_{LES}	Turbulent viscosity, $kg \cdot m^{-1} \cdot s^{-1}$
Δ	LES filter width, m
$\bar{\rho}$	Filtered density, $kg \cdot m^{-3}$
ρ_∞	Density of air, $kg \cdot m^{-3}$
τ	Shear force, $N \cdot m^{-2}$
τ_{mix}	Mixing time, s
τ_{chem}	Chemical time scale, s
δx	Indicator of grid resolution

Subscripts:

i, j, k	Three directions in co-ordinates
g	Growth
d	Decay

INTRODUCTION

Performance-based fire protection design is one of the most widely used engineering approaches to reduce the damage and devastating disasters caused by fire in structures. Fire simulation is used to determine the damage to the structure and measure the values such as smoke spread, temperature distribution, visibility and the amount of carbon monoxide in the environment, which are necessary for the safe evacuation of people from the structure during the development and propagation of the fire. These design methods give also direction to the building design at the point of taking passive fire precautions and determining escape distances. Combustion characteristics of materials including n-heptane and generation of fire products were investigated in detail in the literature (Tewarson, 1986; Khan et al., 2015).

A pool fire is defined as the turbulent diffusion fire burning above a horizontal pool of vaporizing hydrocarbon fuel where buoyancy is the controlling transport mechanism (Sudheer, 2013). The early works on liquid pool fires were performed by Blinov and Khudiakov (1957). Hottel (1959) and Hall (1973) studied the rates of burning of pools of hydrocarbon liquids for different diameters. Yao et al. (2013) developed a new modeling approach of n-heptane pool fire and validated by experimental data. Bordbar and Hostikka (2019) numerically obtained the spectral characteristics of radiation coming from a pool fire flame. Dobashi et al. (2016) performed experiments for small and middle scale n-heptane pool fires to understand the mechanisms of the flame height growth at fire whirls. Yin et al. (2013) built

an altitude chamber where they configured different dynamic pressure descent rates to simulate n-heptane pool fire behaviors under different low pressures. Burning rate, flame height, and fuel temperature distribution of small scale thin-layer n-heptane pool fires were experimentally studied for different pool diameters by Kang et al. (2010). Xin et al. (2002, 2005a, 2005b, 2005c) used FDS software to work on various pool fire scenarious. Hietaniemi et al. (2004) studied on several diameter of n-heptane pool fires.

In order to obtain reliable fire simulation results, reliable fire design curve and input parameters are essential. In this sense, there are various studies in the literature (Staffansson, 2010; Ciani and Capobellin, 2018; Baek et al., 2017; Ingason, 2009; Drysdale, 2011). Also Numajiri and Furukawa (1998) proposed a mathematical expression of the heat release rate curve by a simple equation. New fire design curves were suggested for the utilization in fire simulations (Baek et al., 2017, 2018).
Literature study indicates a lack of knowledge about the small scale (≤ 10cc) n-heptane pool fire. In this study, a 1/100 scale model of a real metro station was built and heat release rate, temperature distribution and visibility were investigated experimentally and numerically with zero piston effect condition along the station. Fire Dynamics Simulator (FDS v6.7.5) software was used to simulate an n-heptane pool fire development by means of available design fire curves in the literature to obtain the closest results to the experimental data.

The aim of this study is to select most suitable fire design curve and make the numerical study independent of the experimental results by not using the experimental results as numerical analysis input for small scale hydrocarbon pool fires.

EXPERIMENTAL SETUP

The model is a scale of the Maltepe Station on Ankaray Metro line located in Ankara/Turkey with a scale of 1:100. The Maltepe Station, built with the cut-and-cover method, has a 90 m platform and rectangular cross-section connection tunnels. In the design of the model, platform length was taken as the characteristic length to be scaled. The model consists of three sections: inlet tunnel, station and outlet tunnel. The model constructed with heat resistant 5 cm thick autoclaved aerated concrete block. The ceiling and floors are covered with a 1 cm thick fiber-resin composite layer. In addition, the interior and exterior of the model were plastered in four layers with fireproof, heat-insulating plaster. Heat resistant glass was used on the symmetry plane to view experiments. Variable frequency driven fan located on the inlet tunnel was used to provide different inlet flow velocities. Besides, a honeycomb mesh was located on the inlet tunnel in order to maintain uniform airflow. The experimental setup of metro station consists of 3 rectangular sections including 900 mm x 324 mm x 220 mm (LxWxH) station and 1000 mm x 120 mm x 120 mm (LxWxH) inlet and outlet tunnels as can be seen in Fig. 1 (Berberoğlu, 2008).

During the experiments, the temperatures inside the station were measured by means of a K-type thermocouple located 5 cm above the 10 cm x 5 cm x 4 mm (LxWxH) in size. The pool contains 10 ml n-heptane fuel.

NUMERICAL MODEL

In the present study, Fire Dynamics Simulator (FDS v6.7.5) software was used to simulate an n-heptane pool fire development under different design fire curves. FDS is a computational fluid dynamics (CFD) model of fire-driven fluid flow, which was developed by the National Institute of Standards and Technology (NIST) (McGrattan et al., 2021a). FDS numerically solves low-speed, thermally driven flows, with an emphasis on smoke and heat transport from fires using Navier-Stokes equations (McGrattan et al., 2021a). Based on Navier–Stokes equations and Large Eddy Simulation (LES) model for turbulent flow, the governing equations are presented on the next section.

Figure 1. (a) Front and (b) rear view of the experimental setup

Computational Domain and Mesh Structure

The computational domain as shown in Fig. 2 consists of three rectangular sections including 900 mm x 324 mm x 220 mm (LxWxH) station and 1000 mm x 120 mm x 120 mm (LxWxH) inlet and outlet tunnels.

In the present study, n-heptane was used as fuel. The FDS fuel library was used to set the physical and chemical properties. HRRPUA (heat release rate per unit area) approach was used in the study and the agreement with experimental data was analysed. Four thermocouples were placed at the middle and T1:35 mm, T2:50 mm, T3:120 mm and T4:205 mm above the pool in order to trace temperature variations.

The ratio D*/ δx is an indicator of grid resolution where D* is the characteristic fire diamater and δx is the size of a grid cell. The ratio of 5 to 10 usually produces favorable results at a moderate computational cost (Nureg 1824, 2007), (McGrattan et al., 2021b). D* is given as

$$D^* = \left(\frac{\dot{Q}}{\rho_\infty C_p T_\infty \sqrt{g}}\right)^{2/5} \quad (1)$$

where $\dot{Q}$ is heat release rate (HRR), ρ_∞ is density of the air, T_∞ is temperature of the air, C_p is specific heat of the air, and g is acceleration of gravity (9.81 m/s^2). Based on Eq. (1), D* is calculated as 7.8 cm, which corresponds to D*/dx = 5 for 1.56 cm and D*/dx = 10 for 0.78 cm cell size (dx), respectively.

The Governing Equations and Boundary Conditions

The finite difference method has been employed in the solution of the three dimensional, time-dependent conservation equations of mass, momentum, energy and species.

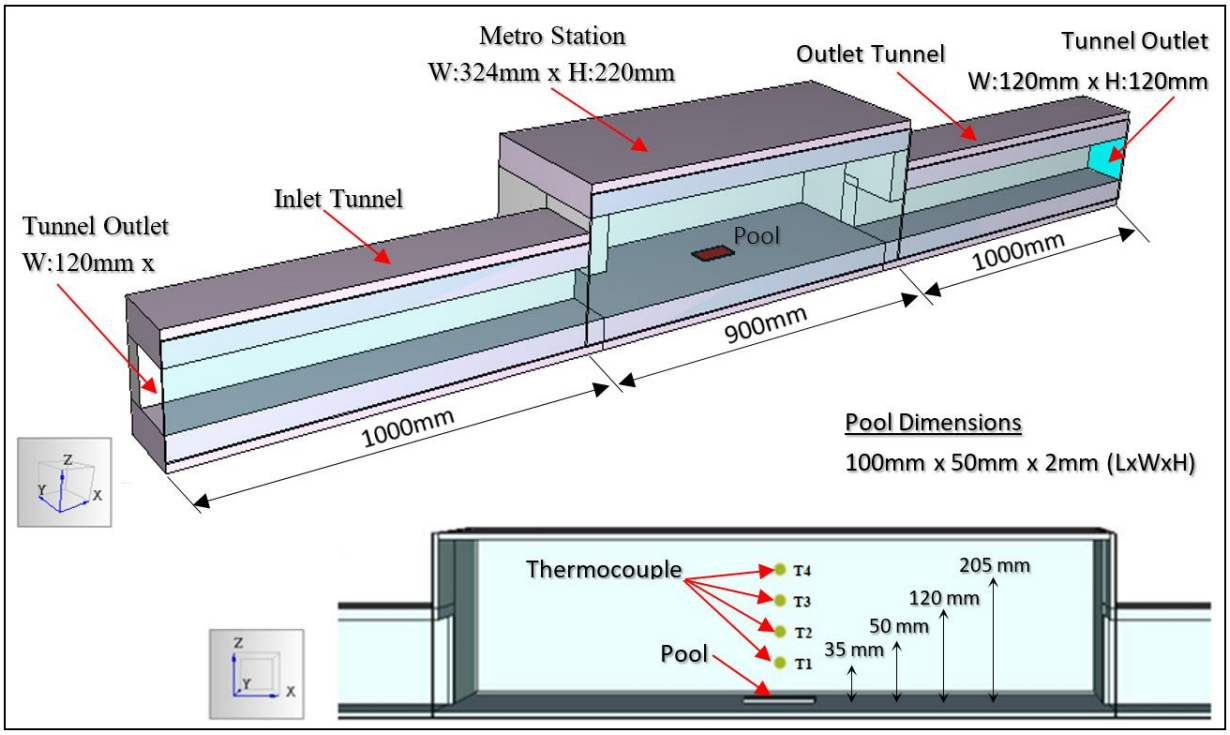

Figure 2. Computational model of the metro station

Thermal distribution and air flow are simulated by solving conservation equations. The filtering operation is applied to the three–dimensional time–dependent Navier–Stokes equations in order to remove the small turbulent scales of the total flow field and to obtain the filtered conservation equations to conduct large–eddy simulations (Aybay, 2010). The Favre–filtered conservation equations can be written as follows:

Conservation of mass:

$$\frac{\partial \rho}{\partial t} + \frac{\partial \bar{\rho}\tilde{u}_j}{\partial x_j} = 0 \tag{2}$$

Conservation of momentum:

$$\frac{\partial \bar{\rho}\tilde{u}_i}{\partial t} + \frac{\partial}{\partial x_j}\left(\bar{\rho}\tilde{u}_i\tilde{u}_j\right) = -\frac{\partial \bar{p}}{\partial x_i} - \frac{\partial \bar{\tau}_{ij}}{\partial x_j} - \frac{\partial \tau_{ij}^{sgs}}{\partial x_j} + \bar{\rho}g_i + \bar{f}_{d,i} + \overline{\dot{m}_b'''}\tilde{u}_{b,i} \tag{3}$$

Conservation of energy:

$$\frac{\partial(\bar{\rho}\tilde{h})}{\partial t} + \frac{\partial\left(\bar{\rho}\tilde{u}_j\tilde{h}\right)}{\partial x_j} = \frac{D\bar{p}}{Dt} - \frac{\partial q_j^r}{\partial x_j} + \frac{\partial}{\partial x_j}\left(k_c\frac{\partial \tilde{T}}{\partial x_j}\right) + \frac{\partial}{\partial x_j}\sum_l\left(\bar{\rho}\,D_l\tilde{h}_l\frac{\partial \tilde{Y}_l}{\partial x_j}\right) \tag{4}$$

Conservation of species:

$$\frac{\partial(\bar{\rho}\tilde{Y}_l)}{\partial t} + \frac{\partial\left(\bar{\rho}\tilde{u}_j\tilde{Y}_l\right)}{\partial x_j} = -\frac{\partial}{\partial x_j}\left(\overline{\rho u_j Y_l} - \bar{\rho}\tilde{u}_j\tilde{Y}_l\right) + \frac{\partial}{\partial x_j}\left(\overline{\rho D_l\frac{\partial Y_l}{\partial x_j}}\right) + \overline{\dot{w}_l} \tag{5}$$

where k_c is the thermal conductivity, $\bar{\rho}$ is the filtered density, q^r is the radiative heat flux, D_l is the material diffusivity, $\tilde{Y}_l$ is Favre-filtered mass species concentration, $\tilde{h}$ is the Favre-filtered enthalpy, $\tilde{u}$ is the Favre-filtered velocity, $\overline{\dot{w}_l}$ is the Favre-filtered species source term and Dp/Dt is the material derivative. The Favre-filtered quantities are denoted by $\widetilde{\emptyset} = \overline{\rho\emptyset}/\bar{\rho}$.

FDS major features in its default operation were used for simulations in the present study (McGrattan et al., 2021a). This major features are large-eddy simulation (LES), low Mach number flow, explicit, second-order discretization, kinetic-energy-conserving numerics, lumped species method, deardoff eddy viscosity subgrid scale closure, constant turbulent Schmidt and Prandtl numbers, simple immersed boundary method for treatment of flow obstructions, eddy dissipation concept (fast chemistry) for single-step reaction between fuel and oxidizer, gray gas radiation with finite volume solution to the radiation transport equation and the rest of simulation parameters and boundary conditions are given in Table 1. In Table 1, U represents the overall heat transfer coefficient calculated based on local regulation for thermal insulation requirements for buildings (TS 825, 2013).

Table 1. Simulation parameters and boundary conditions

Surface Boundary Conditions	Wall: U=1.228 W/m^{2}K, u=v=w=0 Ceiling: U=1.033 W/m^{2}K, u=v=w=0 Floor: U=0.954 W/m^{2}K, u=v=w=0 Glass: U=5.700 W/m^{2}K, u=v=w=0
Tunnel Outlets Boundary Conditions	$\frac{\partial P}{\partial x} = 0$, $\frac{\partial T}{\partial x} = 0$, $\frac{\partial u}{\partial x} = \frac{\partial v}{\partial x} = \frac{\partial w}{\partial x} = 0$
Environment Temperature	21°C
Grid	Structured, uniform, staggered grid
Soot Yield	0.037 kg/kg
CO Yield	0.01 kg/kg
Fuel	Heptane (C_7H_{16})
Fuel Volume	10cc
Pool Dimension	0.1 m x 0.05 m x 0.004 m (LxWxH)
HRR	1.89 kW

Turbulence Model

Turbulence model means the closure for sub-grid scales flux terms in LES. In order to close both the SGS momentum and scalar flux terms, the gradient diffusion is the turbulence model used in FDS. There are two turbulent transport coefficients: turbulent viscosity and the turbulent diffusivity. Turbulent viscosity is a mixing ratio that allows predicting the net effective mixing between species and fluids at sub-grid scales that cannot be resolved. The mesh size determines the smallest eddy scale that the software can resolve. To estimate the net effective mixing in each smaller cells, turbulent viscosity μLES is determined and multiplied by the velocity gradient of the fluid surrounding the cell. In order to obtain the turbulent diffusivity the constant Schmidt number and Prandtl number are used. In the present study the turbulent viscosity μLES and turbulent kinetic energy ksgs are obtained based on the Deardorff model, which are given as follows (McGrattan et al., 2021a):

$$\mu_{LES} = \rho C_V \Delta \sqrt{k_{sgs}} \tag{6}$$

$$k_{sgs} = \frac{1}{2}\left(\left(\bar{u} - \hat{\bar{u}}\right)^2 + \left(\bar{v} - \hat{\bar{v}}\right)^2 + \left(\bar{w} - \hat{\bar{w}}\right)^2\right) \tag{7}$$

$\hat{\bar{u}}$, $\hat{\bar{v}}$, and $\hat{\bar{w}}$ are weighted average of u, v, and w over the adjacent cells, respectively.

Combustion Model

FDS uses mixing-controlled, infinitely fast combustion model. The turbulence-chemistry interaction is handled with partially-stirred batch reactor model which is implemented in each computational cell where only the mixed composition can react. Here concentration is computed for each species and mixing degree. Reactant species are converted to product species at a rate determined by a characteristic mixing time, τmix expressed as follows (McGrattan et al., 2021a):

$$\tau_{mix} = \max(\tau_{chem}, min(\tau_d, \tau_u, \tau_g, \tau_{flame})) \tag{8}$$

Physical processes associated with sub-grid scale (SGS) advections, molecular diffusion, and the buoyant acceleration are involved in Eq. (8).

Chemical time scale, τ_{chem}, is given as

$$\tau_{chem} \sim D_F/(S_L)^2 \tag{9}$$

Molecular diffusion time scale, τ_d, is

$$\tau_d = \frac{\Delta^2}{D_F} \tag{10}$$

Turbulent advection mixing time scale, τ_u, is expressed as

$$\tau_u = \frac{C_u \Delta}{\sqrt{(2/3)k_{sgs}}} \tag{11}$$

Buoyant acceleration mixing time scale, τ_g, is

$$\tau_g = \sqrt{2\Delta/g} \tag{12}$$

where SL is the flame spread, DF is the diffusivity of the fuel, Δ is the LES filter width, Cu is the time scale constant, g is the acceleration of gravity (9.81 m/s^2), and τflame is the acceleration controlled mixing time scale for highly turbulent flames which is neglected since grid spacings stay within a quarter of the minimum flame dimension according to Heskestad correlation given below (McDermott et al., 2011).

$$\frac{L_f}{D} = 3.7(Q^*)^{2/5} - 1.02 \quad (13)$$

$$Q^* = \frac{\dot{Q}_c}{\rho_\infty C_p T_\infty \sqrt{gD}D^2} \quad (14)$$

where L_f is the flame height, D is the effective diameter of the base of the plume, Q^* is the fire Froude number, and $\dot{Q}_c$ is the global heat release of the plume. Ambient values for temperature, specific heat, and density are taken to be T_∞=293 K, C_p=1.01 kJ/kg·K and ρ_∞=1.20 kg/m^3, respectively.

Grid Sensitivity Analysis

The studied cell sizes and the total number of cells are given in Table-2. Mesh number 3 (D*/dx = 10) has been selected which produces favorable results at a moderate computational cost.

Figure 3 shows the comparison of the predicted temperature variation 5 cm above the fire source with respect to time using four different grid resolutions, i.e., the coarse grid with cell size of 1.5 cm, the medium grid with cell size of 1.0 cm, the fine grid with cell size of 0.75 cm, and the extra-fine grid with cell size of 0.6 cm. The predictions with the coarse grid were found to have the largest discrepancies with the other grid resolutions. The results obtained with the fine grid, as employed in the present study, were found to be reasonably close to the predictions with the medium and extra-fine grid results. Therefore, the fine grid was chosen for the present study.

Table 2. Mesh descriptions

Mesh No	Cell Size [cm]	Number of Cell			
		Inlet Tunnel	Metro Station	Outlet Tunnel	Total
1	1.50	9648	23424	9648	42720
2	1.00	32400	79488	32400	144288
3	0.75	76608	188928	76608	342144
4	0.60	150300	367200	150300	667800

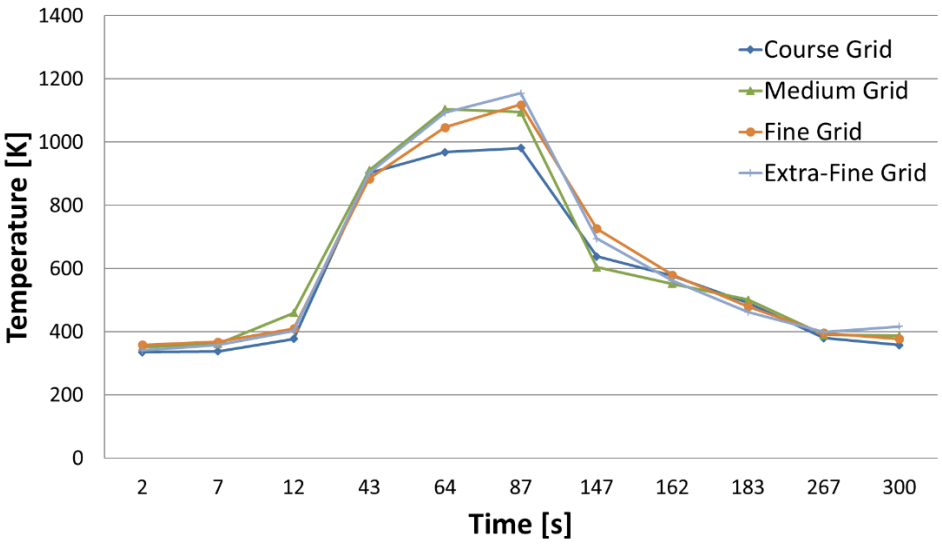

Figure 3. Grid sensitivity analysis

DESIGN FIRE CURVE

Performance-based design with numerical simulation is one of the engineering approach to reduce the loss of life and property due to fire. Validated user defined inputs such as turbulence parameters, radiation parameters, and fire development curve should be used in order to obtain reliable fire simulation results. The fire curve is generally expressed as the variation of temperature or heat release rate (HRR) over time. The main phases are defined as growth, fully developed and decay shown in Fig. 4.

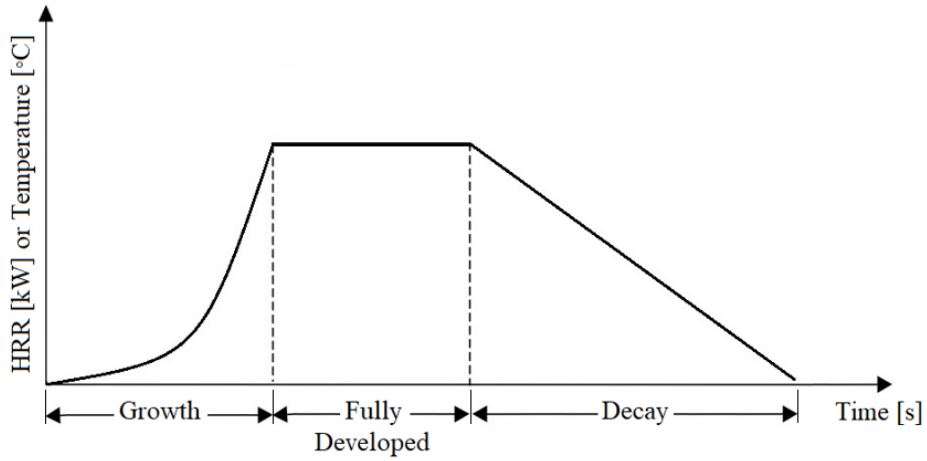

Figure 4. Typical schematic fire design curve

Table 3. Design fire curves used in the study

Case Number	Fire Development		
	Growth	Fully Developed	Decay
1	t^2 (NFPA 204, 2015)	Linear	t^2 (NFPA 204, 2015)
2	tanh (McGrattan et al., 2021c)	Linear	t^2 (NFPA 204, 2015)
3	Eurocode 1 (BS EN 1991-1-2, 2002)	Linear	t^2 (NFPA 204, 2015)
4	Exponential (Ingason, 2009)		
5	Quadratic (Ingason et al, 2015)	Linear	Exponential (Ingason, 2009)

Fire growth is composed of the processes of ignition, flame spread, and burning rate (Quintiere, 1997). Fully developed phase starts when the growth phase has reached its maximum and continues up to combustible materials become run out. The final and usually the longest phase of fire named decay is characterized a significant decrease in fuel or oxygen, putting an end to the fire. Design fire curves can be linear, quadratic or exponential (Baek et al., 2017).

The design fire curve should be able to reflect the characteristics of the overall fire. Besides that, in particular, it is important to predict the behavior of the growth phase to ensure fire safety. Based on this information, depending on the type of fire, the activation temperature of fire protection equipment such as heat detectors and sprinklers can be decided. Fire development is also important to foreseen evacuation times in metro stations and time required for the fire brigade to arrive at the scene, respond to the fire. In this study, several types of design fire curves in the literature (BS ISO-TR 13387-2 1999), (Ingason, 2009), (NFPA 204, 2015), (BS EN 1991-1-2, 2002) were used in numerical analysis to obtain the closest results to the experimental data. Design fire curves used in the study are tabulated and given on the Table 3.

t^2 fire curve

The heat release rate (HRR) in the fire growth phase is commonly expressed as follows. $\dot{Q}$ is the HRR (kW), t is the time after ignition (s), and α is the fire growth rate (kW/s^2).

$$\dot{Q} = \alpha . t^2 \quad (15)$$

tanh fire curve

If the characteristic ramp-up time of the heat release rate per unit area which is defined as TAU_Q in FDS is greater than zero then the ramp up can be defined as tanh (1/τ) at the software (McGrattan et al., 2021c). Hyperbolic tangent is a hyperbolic function that is the ratio of sinh to cosh. It was observed that the growth phase of the fire curve obtained from the experimental results is similar to the tanh curve development.

It is assumed that the fire starts to decay when 80% of the fuel has been consumed as per International Fire Engineering Guidelines (2005) and Staffansson (2010).

In this study, the α_g, α_d, t_g and t_d values used in the numerical analysis of the t^2 and tanh curves were calculated with the help of experimental results given in Fig. 5.

Eurocode 1 fire curve

Eurocode 1 hydrocarbon curve (BS EN 1991-1-2, 2002) was used at the growth phase of the Case 3 as indicated on Table 3. The curve of the growth phase was created by finding the temperature values for each second for 65 seconds. The development of the Hydrocarbon (HC) fire temperature curve is described by the following equation (BS EN 1991-1-2, 2002).

$$T = 20 + 1080(1 - 0.325e^{-0.167t} - 0.675e^{-2.5t}) \quad (16)$$

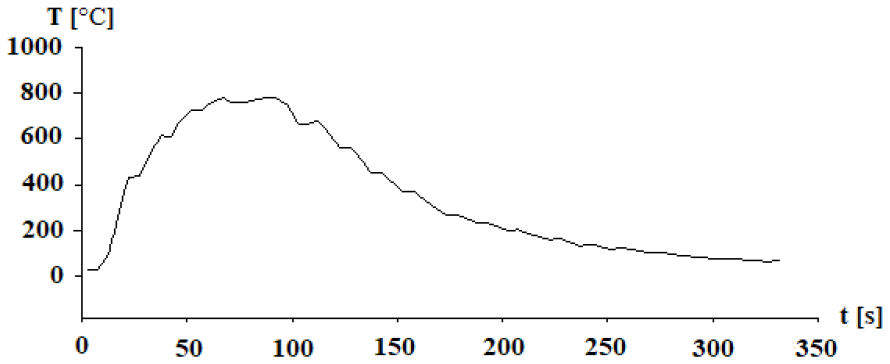

Figure 5. 10cc n-heptane pool fire temperature-time graph measured from T_2 point (Berberoğlu, 2008).

Exponential fire curve

Ingason (2009) suggested a single exponential function for fire design, instead of evaluating the fire development in three separate time phases. Ingason's (2009) fire design is based on Numajiri and Furukawa's works (1998) and it is only applicable to fuel-controlled fires with a small or negligible constant maximum heat release rate period. Q˙_max is the maximum HRR (kW), Etot is the total calorific value (kJ), and n is the retard index. With the help of these parameters, the time to total fire duration td (s), and the time to reach maximum HRR, tmax (s), were calculated. Other parameters r and k are calculated based on Q˙_max and Etot (Ingason, 2009). The time dependent HRR (Q˙(t)) can be calculated with the following equation:

$$\dot{Q}(t) = \dot{Q}_{max} . n . r . (1 - e^{-k.t})^{n-1} . e^{-k.t} \quad (17)$$

where k shows the time width and is calculated as follows:

$$k = \frac{\dot{Q}_{max}}{E_{tot}} . r \quad (18)$$

In Eq. (17) r and n represent the amplitude and retard index, respectively. The amplitude could be obtained as follows:

$$r = (1 - \frac{1}{n})^{1-n} \quad (19)$$

$$n \approx 0.74294 e^{(2.9 \dot{Q}_{max} t_{max} / E_{tot})} \quad (20)$$

t_{max} and t_d are calculated by the following equations:

$$t_{max} = \frac{\ln(n)}{k} \quad (21)$$

$$t_d = \frac{1}{k}\ln\left(\frac{1}{1-\beta_d^{(1/n)}}\right) \quad (22)$$

where

$$\beta_d = E_{tot,t_d}/E_{tot} \quad (23)$$

and E_{tot,t_d} is integrated energy at time td.

Quadratic fire curve

A time-dependent design fire curve for various road tunnel fires with a quadratic growth from zero to time tmax was proposed by Ingason (Ingason et al., 2015). The design curve includes quadratic grow, constant maximum HRR value to the time to decay t_D and an exponential decrease from the maximum HRR value to zero. Time dependent HRR, time to reach maximum HRR t_{max} (s) and time to start of decay period t_D (s) can be calculated with the following equations (Ingason et al., 2015).

$$\dot{Q}(t) = \propto_{g,q} \cdot t^2 \ (t \le t_{max}),\ \dot{Q}(t) = \propto_{g,q} \cdot t_{max}^2 \ (t_{max} < t < t_D),$$
$$\dot{Q}(t) = \dot{Q}_{max} e^{-\alpha_{D,q}(t-t_D)} \ (t \ge t_D) \quad (24)$$

$$t_{max} = \sqrt{\frac{\dot{Q}_{max}}{\alpha_{g,q}}} \quad (25)$$

$$t_D = \frac{E_{tot}}{\dot{Q}_{max}} + \frac{2}{3}t_{max} - \frac{1}{\alpha_{D,q}} \quad (26)$$

Since the maximum HRR is very low (Q_{max}=1.89 kW), the time to decay obtained as negative value from the Eq. (22). Therefore, the quadratic curve was not included in the comparison study.

RESULTS AND DISCUSSION

Numerical simulations were performed with the Fire Dynamics Simulator (FDS v6.7.5) for an n-heptane pool fire in a 1:100 scaled metro station model based on the experimental study of Berberoğlu (2008) to evaluate the prediction performance of quadratic, exponential, linear, t^2 and combination of design fire curves. In addition, it was aimed to perform numerical analysis and determine the most appropriate parameters and fire curves for predicting small scale pool fires without using experimental data.

Design fire curves implemented in the FDS code are shown in Fig. 6. The t^2, tanh and exponential curves have been dimensionalized by using instantaneous HRR over peak HRR, and for Eurocode curve by using instantaneous temperature over maximum temperature. The values of the fire growth rate α for growth and decay phases of the fire curve have been taken from experimental data. It was observed that Eurocode and tanh curves were more compatible with the curve obtained from the experimental results.

Detailed results obtained for different fire development curves have been presented in this part of the study. First of all, the numerical results have been validated with experimental results. Fig. 7 shows the time-temperature curves obtained for mentioned fire designs and experimental result. The data have been obtained 5 cm above the pool.

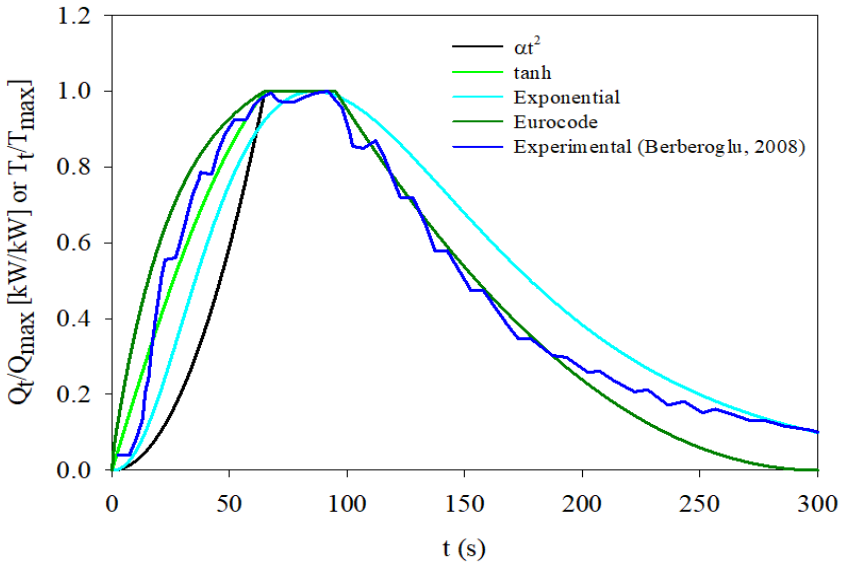

Figure 6. Design fire curves

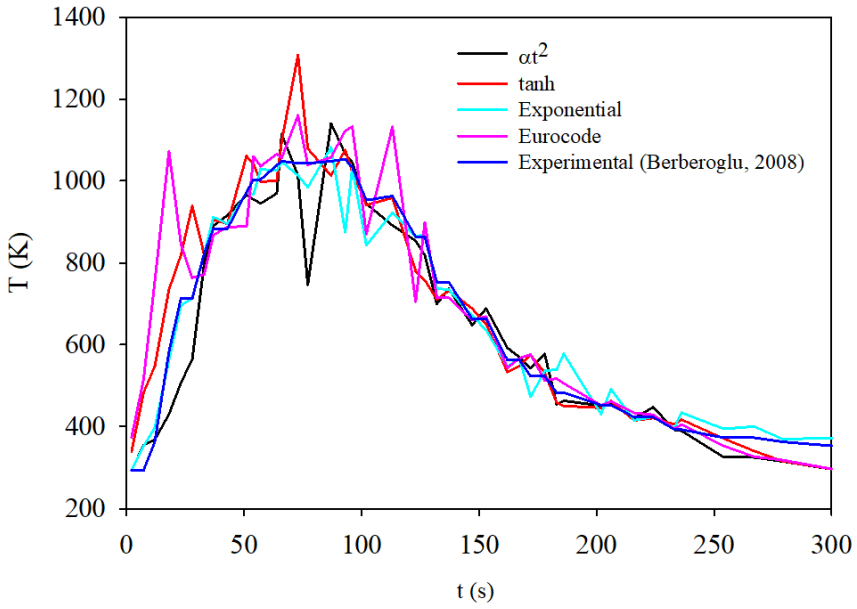

Figure 7. Time-temperature curves for numerical and experimental results

The predictions with αt2, tanh and exponential design curves are reasonably good agreement with each other and with the experimental data. Accordingly, it has been observed that the most suitable fire design curve was obtained as the exponential design curve which showed an average difference of 4.59% with the experimental results. It has been seen that the t^2 and tanh curves have acceptable differences of 6.92% and 9.02%, respectively, and the Eurocode HC is less suitable than the other curves with a difference of 12.17%. It is also stated in the literature that the exponential curve gives good results in pool fires with a short or negligible fully developed phase (Numajiri and Furukawa, 1998, Ingason, 2009, Ingason et al, 2015).

The experimental and numerical analysis results obtained from T1, T3 and T4 thermocouple positions given in Fig. 2 are compared in Fig. 8. The numerical data obtained using the exponential fire development curve were found to be in agreement with the test results. Since the T1 thermocouple is just above the fire and the graph reflects the instantaneous data, oscillation was observed in the numerical results. In the experimental study, it is seen that the oscillation is low because the measurements were taken at longer intervals.

The time – HRR curves obtained using different design curves are given in Fig. 9. Accordingly, it is understood that all results are compatible with each other. However, as it is observed in Fig. 9, it is seen that the Eurocode curve and Exponential curve are of higher order than the other curves in the development and decay phase, respectively.

Temperature distributions along the station at the level of z=205 mm and z=120mm above the floor are obtained from numerical analysis and given in Fig. 10. It is seen that the temperature distribution is higher on the upper plane and reaches up to 720 K. Also it is observed that minimum temperature on the occupied zone is around 480 K which is higher than the tenability temperature.

The temperature distribution images obtained along the plane passing through the center of the station at t=80s (peak HRR) by using different fire design curves are given in Fig. 11 below.

It is observed in Fig. 11 that different temperature distributions are obtained especially in the ceiling region of the station by using different fire design curves. It is also observed that high temperature values are more distributed along the ceiling compared with the exponential case. In addition, it is seen that Eurocode 1 curve releases more heat than other curves in the period up to tmax. Hence, it is understood that the fire design selection is important to obtain accurate temperature distribution. This is attributed to fire design curve (Fig. 6) which reaches higher temperatures sooner compared with the other curves.

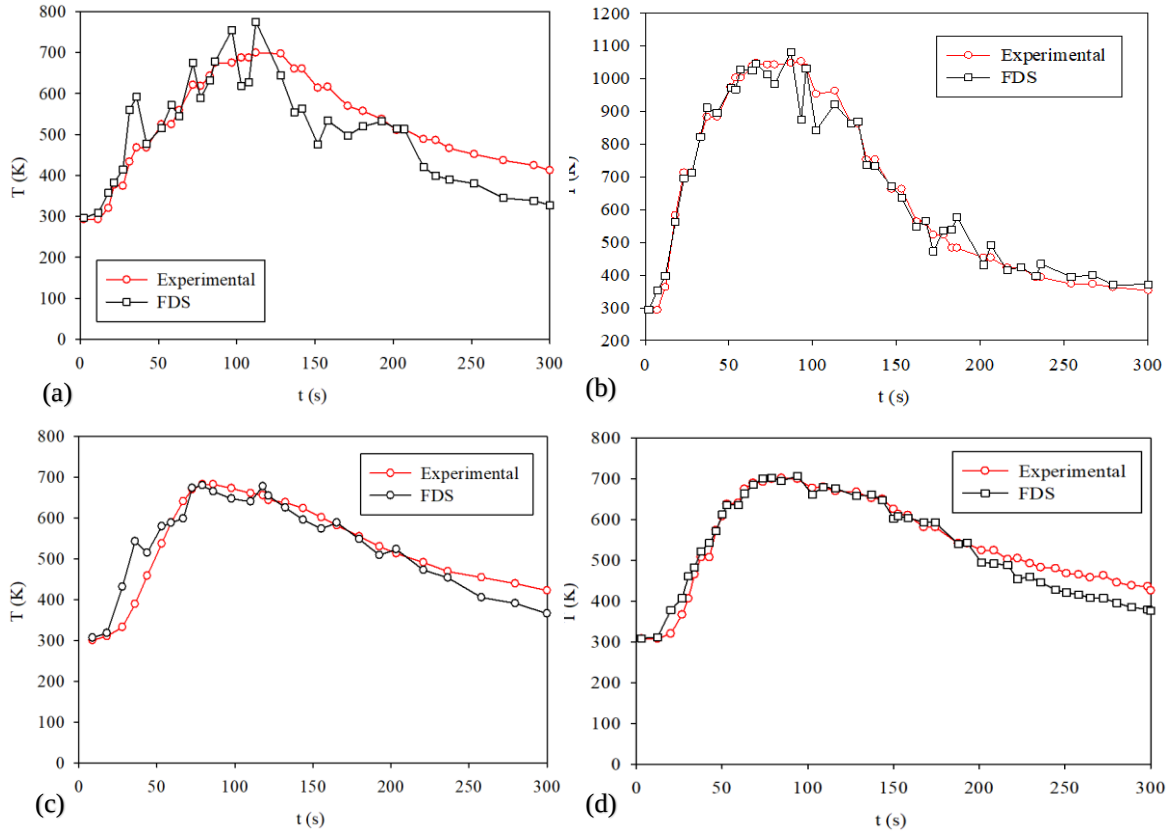

Figure 8. Time-temperature curves for (a) T1, (b) T2, (c) T3, and (d) T4 thermocouple

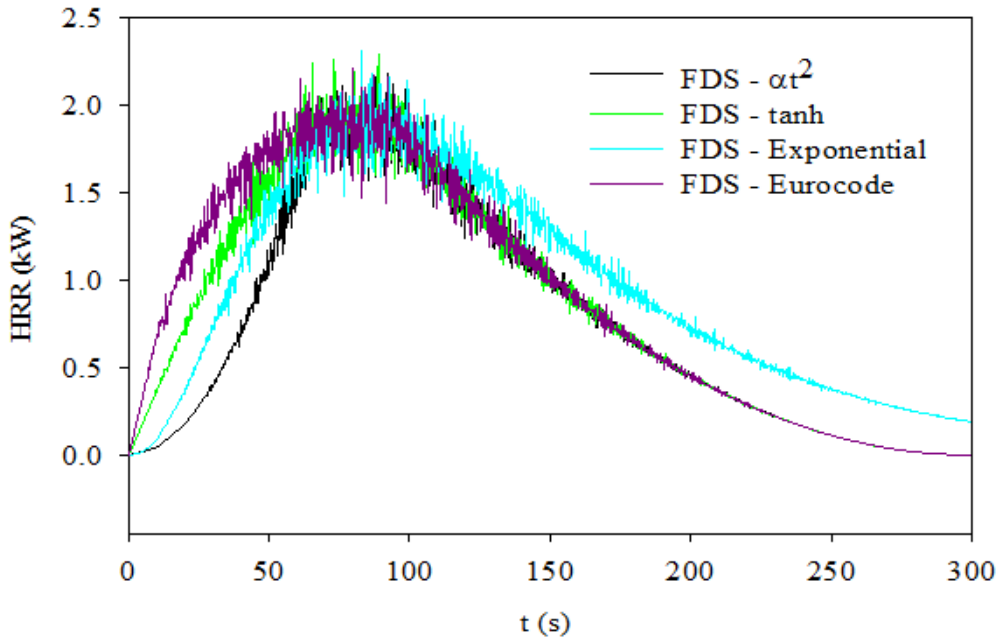

Figure 9. Time-HRR curves for different numerical results

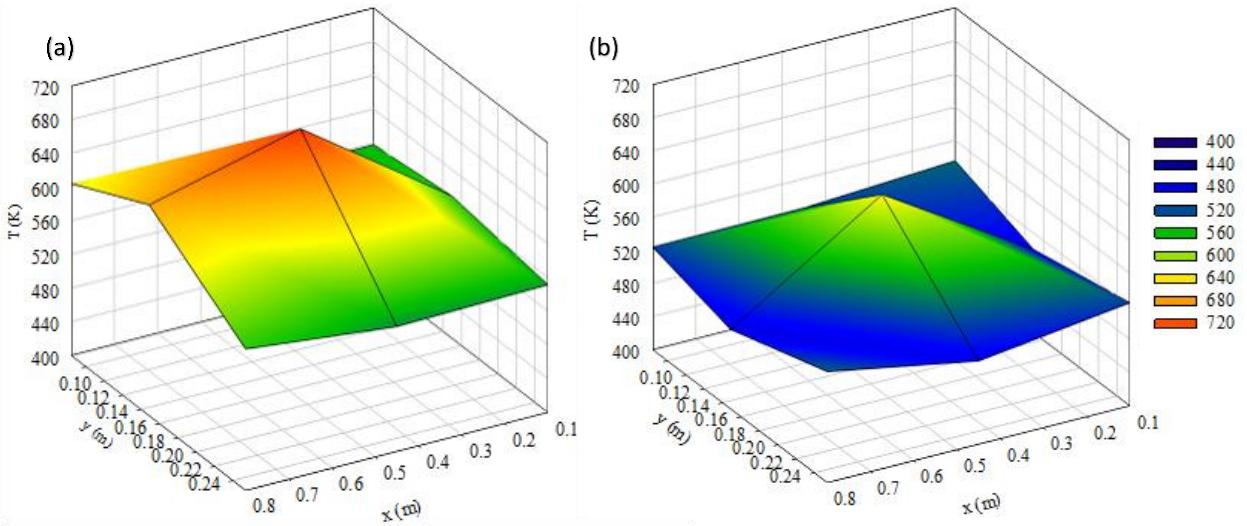

Figure 10. Temperature distributions at the level of z=205 mm (a) and z=120 mm (b) along the station

The soot distributions obtained along the same plane for different time steps by using exponential design curve are given in Fig. 12.

As can be seen from Fig. 12, it is understood that the soot level in the station rises at the 60th second when the combustion comes to peak heat release rate and the soot remains at the same level for 2 minutes, then it is exhausted from the tunnel outlets over time.

The carbon monoxide (CO) content obtained along the same plane for different time steps by using exponential design curve are given in Fig. 13.

According to NFPA 130 (2020) the maximum carbon monoxide exposure should not be more than 1706 ppm for sensitive populations up to four minutes. As can be seen in Fig. 13 the amount of CO at 240 seconds (4th minute) is found to be around 120 ppm and below the value specified in the standard.

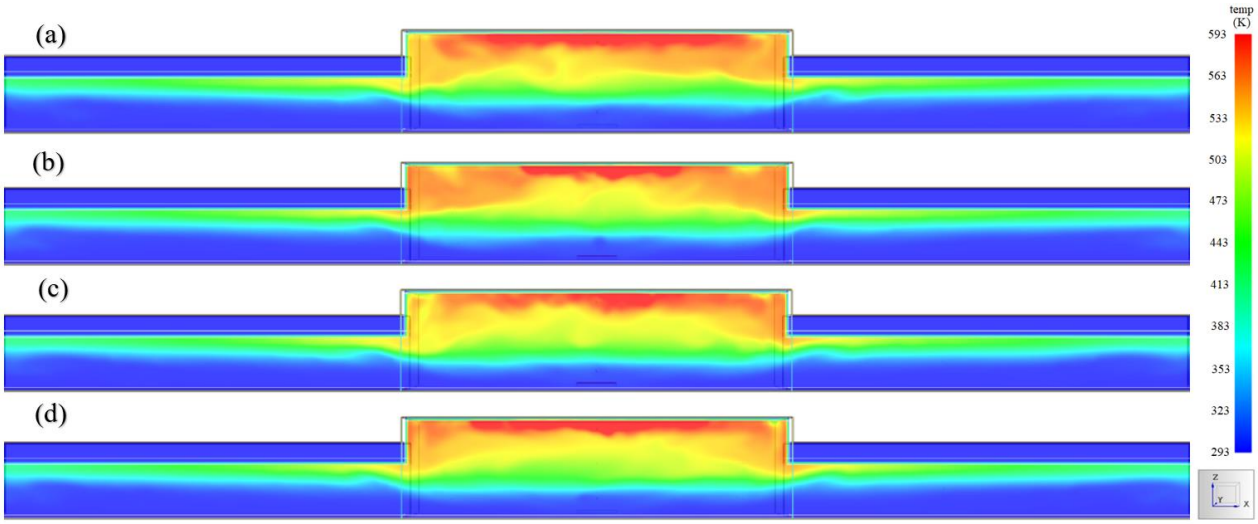

Figure 11. The temperature distribution along the station at the center of the station for (a) αt^2, (b) tanh, (c) exponential, and (d) Eurocode 1 fire curves

Figure 12. The soot distribution along the station during fire

The visibility obtained along the same plane for different time steps by using exponential design curve is given in Fig. 14. According to NFPA 130 (2020), in places where emergency lighting and exit indicators should be discernible at 30 m, and the visibility of doors and walls should be at least 10 m in order not to hinder evacuation. If the visibility is below these values, loss of vision due to smoke could make the occupants lose their sense of direction and thus cause heavier losses. As can be seen in Fig. 14 the visibility is under 10 m after 60 seconds. For this reason, it is understood that a forced ventilation system should be installed in the metro stations.

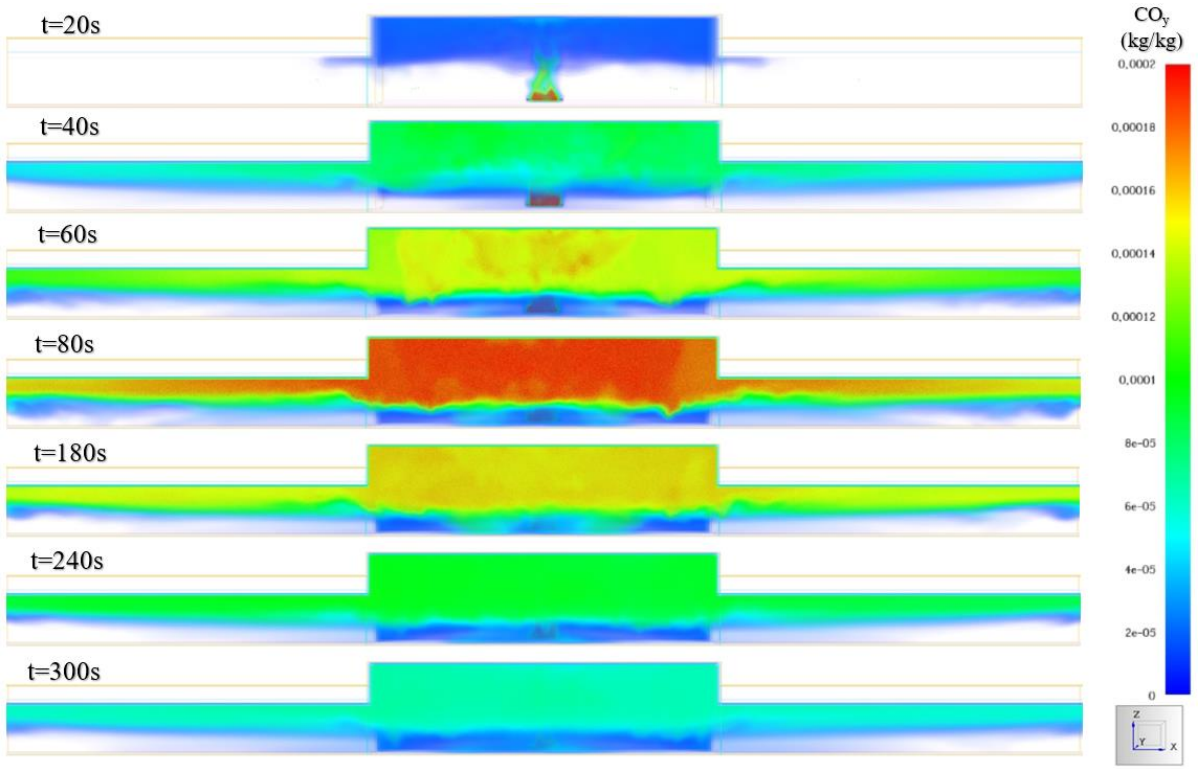

Figure 13. The CO content obtained along the station during fire

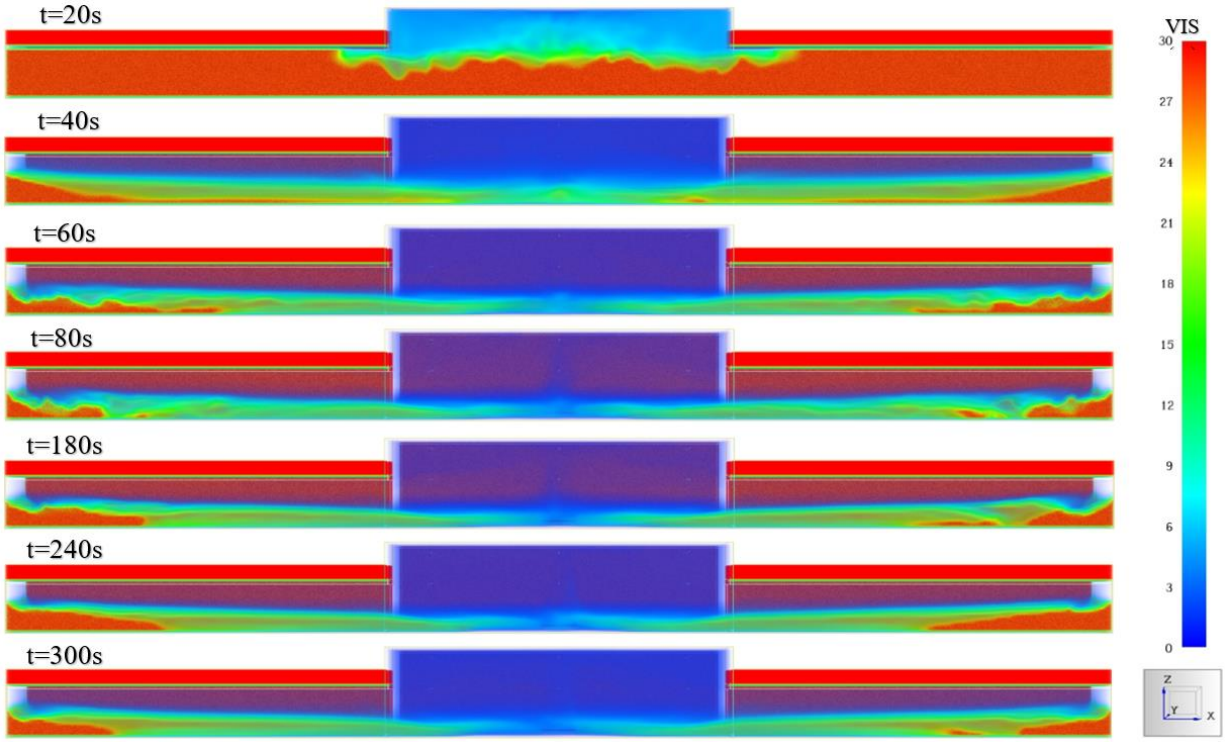

Figure 14. Visibility along the station during fire

CONCLUSIONS

In this study, experimental and numerical simulations are performed for an n-heptane pool fire in a 1:100 scaled metro station model to evaluate the prediction performance of quadratic, exponential, linear, t^2 and combination of the design fire curves. In addition, it is aimed to perform numerical analysis and determine the most appropriate parameters and fire curves for predicting small scale pool fires without using experimental data. The most important conclusions depicted from the findings are presented below:

- The numerical results obtained using FDS are validated with experimental data and good agreement is observed for all design fire curves between 4.59% to 9.02% except Eurocode HC one which is less suitable than the other curves with a difference of 12.17%.

- It is observed that the exponential design fire curve predicted more similarly to the fire growth phase with about 1.2% mean difference measured in the experiment and duration of fire with about 4.49% mean difference better than the design fire curves proposed by other studies.

- Results showed that the visibility is under 10 m after 60 seconds. For this reason, it is understood that a forced ventilation system should be installed in the metro stations.

- It is observed that the carbon monoxide content obtained as 120 ppm, which is far below the tenability limit of 1706 ppm that affect human health in the standards.

- It is seen that the HRR obtained via Eurocode and exponential curves is of higher order than the other curves in the development and decay phase, respectively. It was observed that there was an average difference of 8.4% between the HRR values obtained with the Eurocode and tanh fire development curves.

- Regardless of the experimental results, it is seen that the temperature distribution results obtained from the numerical study using exponential fire design curve and the radiation / turbulence parameters obtained from the literature are found to have an average of 5% difference with the experimental results. Therefore, it can be said that in small scale hydrocarbon pool fires, fire design can be done using exponential design curve.

- Further numerical and experimental works are needed in the future to have in sight of pool fires for different type of fuels and sizes to validate fire design curves.

ACKNOWLEDGEMENTS

The authors of this article declare that the materials and methods used in this study do not require ethical committee permission and/or legal-special permission.

REFERENCES

Australian Government, State and Territories of Australia, *International Fire Engineering Guidelines*, 2005.

Aybay, O., 2010, *Time-Conservative Finite-Volume Method with Large-Eddy Simulation for Computational Aeroacoustics*, Ph.D. Thesis, Durham University, Durham, UK.

Baek, B., Oh, C. B., Lee, E. J., 2017, Nam, D. G., Application Study of Design Fire Curves for Liquid Pool Fires in a Compartment, *Fire Sci. Eng*., 31, 4, 43-51.

Baek, B., Oh, C. B., Lee, C. Y., 2018, Evaluation of Modified Design Fire Curves for Liquid Pool Fires Using the FDS and CFAST, *Fire Sci. Eng*., 32, 2, 7-16.

Berberoğlu, M. İ., 2008, *Fire Modelling and Simulation for Subway Stations*, M.Sc. Thesis, Gazi University Institute of Science and Technology, Ankara, Turkey.

Blinov, V. I. and Khudiakov, G.N., 1957, The Burning of Liquid Pools, *Doklady Akademi Nauk SSSR*, 113, 1094.

Bordbar, H., Hostikka, S., 2019, Numerical Solution of LBL Spectral Radiation of a N-Heptane Pool Fire, *Proceedings of the 9th International Symposium on Radiative Transfer*, RAD-19.

BS EN 1991-1-2 Eurocode 1: Actions on Structures - Part 1-2: General Actions - Actions on Structures Exposed To Fire, 2002.

BS ISO-TR 13387-2 Fire Safety Engineering - Part 2: Design Fire Scenarios and Design Fires, 1999.

Ciani, F., Capobellin, M., 2018, Fire Growth Rate Strategies in FDS, *3rd European Symposium on Fire Safety Science*.

Dobashi, R., Okura, T., Nagaoka, R., Hayashi, Y., Mog, T, 2016, Experimental Study on Flame Height and Radiant Heat of Fire Whirls, *Fire Technol*. 52, 1069–1080.

Drysdale, D., 2011, *An Introduction to Fire Dynamics*, A John Wiley & Sons, University of Edinburgh, Scotland, UK.

Hall, A. R., 1973, Pool Burning: A Review, In Oxidation and Combustion Reviews, Volume 6 (ed. C.F.H. Tipper), 169–225, Elsevier, Amsterdam.

Hietaniemi, J., Hostikka S., and Vaari J., 2004, *FDS Simulation of Fire Spread – Comparison of Model Results with Experimental Data*, VTT Working Papers 4, VTT Building and Transport, Espoo, Finland.

Hottel, H. C., 1959, Review: Certain Laws Governing The Diffusive Burning Of Liquids by Blinov and Khudiakov (1957) (Dokl. Akad. Nauk SSSR, 113, 1096). Fire Research Abstracts and Reviews, 1, 41–43.

Ingason, H., Li, Y. Z., Lönnermark, A., 2015, *Tunnel Fire Dynamics*, Springer, New York.

Ingason, H., 2009, Design Fire Curves for Tunnels, *Fire Safety Journal*, 44, 259–265.

Kang, Q., Lu S., Chen, B., 2010, *Experimental Study on Burning Rate of Small Scale Heptane Pool Fires*, *Chinese Science Bulletin*, 55, 10, 973–979.

Khan, M., Tewarson, A., and Chaos, M., 2015, *Combustion Characteristics of Materials and Generation of Fire Products*, SFPE Handbook of Fire Protection Engineering, 5th ed. Springer, New York.

McDermott, R., McGrattan K., and Floyd, J., 2011, A Simple Reaction Time Scale for Under-Resolved Fire Dynamics. In Fire Safety Science – *Proceedings of the 10th International Symposium*, 809– 820, University of Maryland, College Park, Maryland, USA.

McGrattan, K., Hostikka, S., McDermott, R., Floyd, J., and Vanella M., 2021a, *NIST Special Publication 1018-1 Sixth Edition Fire Dynamics Simulator Technical Reference Guide Volume 1: Mathematical Model*.

McGrattan, K., Hostikka, S., McDermott, R., Floyd, J., and Vanella M., 2021b, *NIST Special Publication 1018-3 Sixth Edition, Fire Dynamics Simulator, Technical Reference Guide VTT Technical Research Centre of Finland, Volume 3: Validation*.

McGrattan, K., Hostikka, S., McDermott, R., Floyd, J., and Vanella M., 2021c, *NIST Special Publication 1019 Sixth Edition, Fire Dynamics Simulator User's Guide*.

NFPA (National Fire Protection Association) 204 - *Standard for Smoke and Heat Venting*, 2015.

NFPA (National Fire Protection Association) 130 - *Standard for Fixed Guideway Transit and Passenger Rail Systems*, 2020.

Numajiri, F., Furukawa, K., 1998, Short Communication: Mathematical Expression Of Heat Release Rate Curve and Proposal of 'Burning Index', *Fire Mater*, 22, 39–42.

NUREG -1824, *Verification and Validation of Selected Fire Models for Nuclear Power Plant Applications*, U.S. Nuclear Regulatory Commission, 2007.

Quintiere, J. G., 1997, *Fire Growth: An Overview*, Fire Technology First Quarter, Department of Fire Protection Engineering, University of Maryland, College Park, USA.

Staffansson, L., 2010, *Selecting Design Fires. Department of Fire Safety Engineering and Systems Safety*, Lund University, Sweden.

Sudheer, S., 2013, *Characterization of Open Pool Fires and Study of Heat Transfer in Bodies Engulfed in Pool Fires*, Ph.D. Thesis, Indian Institute of Technology, Bombay, India.

Tewarson, A., 1986, *Prediction of Fire Properties of Materials Part 1: Aliphatic and Aromatic Hydrocarbons and Related Polymers*, Technical Report NBS-GCR-86-521, National Institute of Standards and Technology, Gaithersburg, MD, USA.

TS 825 Thermal insulation requirements for buildings, TSE Turkish Standard, 2013.

Xin, Y., Gore J. P., McGrattan K.B., Rehm R.G., and Baum H.R., 2002, Large Eddy Simulation of Buoyant Turbulent Pool Fires, *In Twenty-Ninth Symposium (International) on Combustion*, 259–266. Combustion Institute, Pittsburgh, Pennsylvania.

Xin, Y, 2005a, Baroclinic Effects on Fire Flow Field, *In Proceedings of the Fourth Joint Meeting of the U.S. Sections of the Combustion Institute*, Combustion Institute, Pittsburgh, Pennsylvania, USA.

Xin, Y., Gore J. P., McGrattan K. B., Rehm R. G., and Baum H. R., 2005b, Fire Dynamics Simulation of A Turbulent Buoyant flame Using A Mixture-Fraction-Based Combustion Model, *Combustion and Flame*, 141, 329–335.

Xin, Y., and Gore, J. P., 2005c, Two-Dimensional Soot Distributions in Buoyant Turbulent Fires, *In Thirtieth Symposium (International) on Combustion*, Combustion Institute, Pittsburgh, Pennsylvania, USA.

Yao, W., Yin, J., Hu X., Wang, J., Zhang, H., 2013, Numerical Modeling of Liquid -Heptane Pool Fires Based On Heat Feedback Equilibrium, *Procedia Engineering*, 62, 377-388.

Yin, J., Yao, W., Liua, Q., Wua N., Zhoub Z., Wuc Y., Zhang H., 2013, Experimental Study of N-Heptane Pool Fire Behaviors under Dynamic Pressures in an Altitude Chamber, *Procedia Engineering*, 52, 548-556.